Toward Numerically Exact Computation of Conductivity in the Thermodynamic Limit of Interacting Lattice Models

Jeremija Kovačević,[1] Michel Ferrero,[2,3] and Jakša Vučičević[1]
[1]Scientific Computing Laboratory, Center for the Study of Complex Systems, Institute of Physics Belgrade, University of Belgrade, Pregrevica 118, 11080 Belgrade, Serbia
[2]CPHT, CNRS, Ecole Polytechnique, Institut Polytechnique de Paris, Route de Saclay, 91128 Palaiseau, France
[3]Collège de France, 11 place Marcelin Berthelot, 75005 Paris, France

(Received 31 January 2025; accepted 6 June 2025; published 2 July 2025)

Computing dynamical response functions in interacting lattice models is a long-standing challenge in condensed matter physics. In view of recent results, the dc resistivity ρ_{dc} in the weak-coupling regime of the Hubbard model is of great interest, yet it is not fully understood. The challenge lies in having to work with large lattices while avoiding analytical continuation. The weak-coupling ρ_{dc} results were so far computed at the level of the Boltzmann theory and at the level of the Kubo bubble approximation, which neglects vertex corrections. Neither theory was so far rigorously proven to give exact results even at infinitesimal coupling, and the respective dc resistivity results differ greatly. In this Letter we develop, cross-check and apply two state-of-the-art methods for obtaining dynamical response functions. We compute the optical conductivity at weak coupling in the Hubbard model in a fully controlled way, in the thermodynamic limit, and without analytical continuation. We show that vertex corrections persist to infinitesimal coupling, with a constant ratio to the Kubo bubble. We connect our methods with the Boltzmann theory, and show that the latter applies additional approximations that lead to quantitatively incorrect scaling of ρ_{dc} with respect to the coupling constant.

DOI: 10.1103/mm38-zttx

Strongly correlated electronic systems often display rich, yet remarkably universal phase diagrams [1–10]. One of the most puzzling universal phenomena is the strange-metallic linear-in-temperature dc resistivity [9,11–19]. It appears in unconventional and high-temperature superconductors, in the regime where their critical temperature T_c is the highest [1,11,12,16,19]. In other cases, strange metals are associated with quantum critical points [9,17,20–22]. This raises the question of whether there is an intimate connection between criticality, transport properties, and the magnitude of the superconducting T_c. To make sense of the vast experimental data, one must be able to compute the conductivity in interacting lattice models, which is a difficult, long-standing task. The main challenge is to find a way to obtain controlled results on the real frequency axis and, at the same time, avoid finite lattice-size effects. Exact diagonalization based methods [finite-temperature Lanczos (FTLM) [23–25]], linked cluster expansions [26–28], and the density-matrix renormalization group [29] are all inherently limited to small lattice sizes. Quantum Monte Carlo methods, on the other hand, either require analytical continuation [30–32] or are effectively limited to atomic problems [33–37]. In the special case of Hall resistivity, expansions in terms of thermodynamic quantities allow for progress [38,39]. In this Letter, however, we formulate a general and systematic way forward.

The workhorse model for the description of the cuprates (and many other classes of correlated systems) is the Hubbard model [2,7,10,14,21,40–43]. Early works [21] have shown that the infinite-dimensional Bethe-lattice Hubbard model roughly describes the normal phase resistivity in LSCO at moderate to high temperature. However, the physics at low temperature is expected to be dominated by the dimensionality of the model, and thus of primary interest is the Hubbard model on the 2D square lattice. At very strong coupling and high temperature, small 2D lattices become representative of the thermodynamic limit, and FTLM was used to obtain numerically exact results [23,24]. However, to address the questions of strange-metallic behavior and its connection to quantum critical points [1,12,13,16,18,20,22], one must be able to perform computations at lower temperature and, perhaps, lower coupling, a regime where small-cluster methods fail.

Recent works [32,44] have indicated that the ground-state phase diagram of the (nearest-neighbor hopping) square-lattice Hubbard model features a quantum critical line, delineating an ordered stripe ground state. The quantum critical line passes through zero coupling at zero doping (i.e., half-filling). At this point, charge and spin susceptibility diverge [45], and both the Boltzmann theory [46,47] and the Kubo bubble [45] predict a linear-in-temperature resistivity down to the lowest accessible temperature. This finding is in line with numerous

observations of linear resistivity in the vicinity of quantum critical points [12,13,16,18,20,22]. Kiely and Muller [46] have argued that the linear-resistivity strange metal observed at half-filling and weak coupling is connected to the strange metal in the cuprates, corresponding to the strong coupling and finite doping regime of the Hubbard model.

However, our recent results [45] have shown a strong quantitative disagreement between Boltzmann theory and the Kubo bubble, casting doubt on whether either of the theories captures correctly even the qualitative behavior of resistivity. To resolve the phenomenology at weak coupling, better methods are needed.

In this Letter, we address the conductivity in the square lattice Hubbard model. We develop two state-of-the-art methodologies and fully avoid finite-size effects and the uncontrolled analytical continuation [24,31,48].

First, we make use of the real-frequency diagrammatic Monte Carlo (RFDiagMC) [49–52], which relies on constructing a power-series expansion for a given physical quantity; the resulting Feynman diagrams are computed up to a given order and then the series is (re)summed. The imaginary-time integrals in Feynman diagrams are solved analytically (which circumvents analytical continuation), while spatial degrees of freedom are summed over using (quasi) Monte Carlo [36,53,54]. The thermodynamic limit is treated directly.

Next, we devise three different nonequilibrium protocols, where we perturb the system with small external fields and compute the current response as a function of time; we then use the results to reconstruct the optical and dc conductivity in a manner of "inverse linear response theory." In practice, we solve the Kadanoff-Baym equations to obtain the Green's function, given an approximation for the self-energy as input. We do this calculation for lattices as large as 60×60 and confirm convergence of the results with lattice size.

Our diagrammatic series expansion and the corresponding non-equilibrium results are in excellent agreement, which confirms the validity of both implementations. As the coupling constant approaches zero, we observe that vertex corrections to dc conductivity do not vanish, but rather diverge with the same power-law scaling as the Kubo bubble contribution, meaning that they remain quantitatively important even at infinitesimal coupling. Vertex corrections are, however, not very big relative to the Kubo bubble. Nevertheless, neither the Kubo bubble approximation nor the Boltzmann equation yield quantitatively correct results, even at infinitesimal coupling.

Model—We are treating the square lattice Hubbard model. The Hamiltonian reads

$$H = -t\sum_{\langle ij\rangle,\sigma} c^{\dagger}_{\sigma,i}c_{\sigma,j} - \mu\sum_{\sigma,i} n_{\sigma,i} + U\sum_{i} n_{\uparrow,i}n_{\downarrow,i}, \quad (1)$$

where i, j enumerate lattice sites, $c^{\dagger}/c$ are creation or annihilation operators, $\sigma = \uparrow, \downarrow$ denotes spin, t is the nearest-neighbor hopping amplitude, set to $t = 0.25$. The particle-number operator is denoted $n_{\sigma,i} = c^{\dagger}_{\sigma,i}c_{\sigma i}$, and μ is the chemical potential, which is used to tune the average occupancy of the sites. The coupling constant is denoted U. In practice, we absorb the Hartree shift in the chemical potential, $\tilde{\mu} = \mu - U\langle n_{i,\sigma}\rangle$, and thus $\tilde{\mu} = 0$ corresponds to half-filling. We assume $\hbar = e = 1$.

Nonequilibrium approach—We consider the time evolution of the Hubbard model, which was in a thermal state at times $t < 0$, and was then subjected to an external perturbation starting from time $t = 0$. Given an approximation for the self-energy, the Green's function can be computed by solving the Kadanoff-Baym equations [we use the code package NESSi [55] and cross-check with our own implementation; see Supplemental Material (SM) [56] for details]. Kadanoff-Baym equations are formulated on the three-piece time contour as [57]

$$G(t,t')[-i\overleftarrow{\partial}_{t'} - h(t')] - \int_{\mathcal{C}} \mathrm{d}\bar{t}\, G(t,\bar{t})\Sigma(\bar{t},t') = \delta_{\mathcal{C}}. \quad (2)$$

Here, G is the full Green's function, Σ is the self-energy, and h is the single-particle Hamiltonian, which introduces an external electric field through the vector potential $\mathbf{A}$, namely $\mathbf{E} = -\partial_t\mathbf{A}$. We restrict ourselves to fields along the x direction [assuming site positions to be $\mathbf{r}_i = (x_i, y_i)$, with $x_i, y_i \in \mathbb{Z}$] and the corresponding longitudinal response [58]. The time-diagonal elements in the lesser component of the Green's function contain information about the uniform current, i.e., $\langle j(t)\rangle = -(i/N)\sum_{\sigma,\mathbf{k}} v_{\mathbf{k}-\mathbf{A}(t)} G^{<}_{\sigma,\mathbf{k}}(t,t)$ [57,59], and $v_{\mathbf{k}}$ is the x component of the velocity of an electron in the plane-wave state $\mathbf{k}$.

On the other hand, the time evolution of the current following application of a weak electric field can be computed based on the knowledge of the retarded current-current correlation function in equilibrium [60], Λ, as

$$\langle j(t)\rangle = \int_{-\infty}^{t} \mathrm{d}t' \Lambda(t-t')A(t') - KA(t), \quad (3)$$

with $K = -\langle E_{\mathrm{kin}}\rangle/2$, i.e., minus the average kinetic energy per site per spatial dimension. The first term is the paramagnetic part of the current; the second term is the diamagnetic part (see SM for details). Alternatively, if one knows the optical conductivity σ, the current response is computed as

$$\langle j(t)\rangle = \int_{-\infty}^{t} \mathrm{d}t' \sigma(t-t')E(t'). \quad (4)$$

The current-current correlation function is related to the optical conductivity through $\sigma(t) = K\theta(t) - \int_0^t \mathrm{d}t'\Lambda(t')$, or $\partial_t\sigma = -\Lambda$ (for $t > 0$). The optical conductivities in time

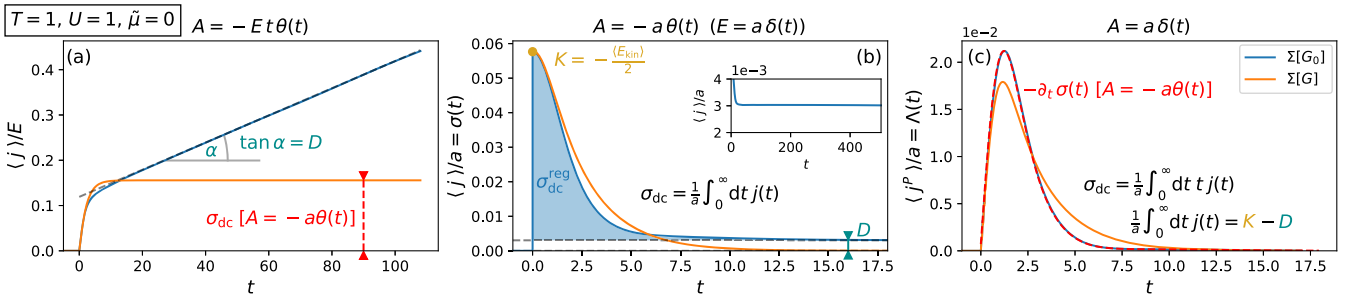

FIG. 1. Example of nonequilibrium, inverse linear response theory. Plots show current response vs time in three different nonequilibrium protocols: (a) constant electric field E, (b) short pulse of electric field, and (c) short pulse of vector potential A. Protocol (a) allows to extract $\sigma_{\rm dc}$; (b) and (c) yield the full $\sigma(t)$ [and thus $\sigma(\omega)$]. Different curves correspond to different self-energy approximations, namely $\Sigma[G]$ and $\Sigma[G_0]$. The red dashed lines in panels (a) and (c) are comparisons with the protocol (b). In protocol (c), we show the paramagnetic part of the current j^p as only this part is relevant. All three protocols yield consistent results. In the $\Sigma[G_0]$ approximation, we observe a finite charge stiffness D. The inset in panel (b) enlarges the long-time tail, showing clearly that $\sigma(t\to\infty)=D$.

and frequency domains are connected via Fourier transformation $\sigma(\omega)=\int_{-\infty}^{\infty}{\rm d}te^{i\omega t}\sigma(t)$, and the dc conductivity is simply $\sigma_{\rm dc}\equiv\sigma(\omega=0)$.

We devise nonequilibrium protocols that will allow us to invert the linear response [Eqs. (3) and (4)] for $\Lambda(t)$ and $\sigma(t)$, compute them based on the current response, and reconstruct $\sigma(\omega)$. The three protocols are (a) constant electric field, (b) short pulse of electric field and (c) short pulse of vector potential. The corresponding expressions for the vector potential $A(t)$ are given in Fig. 1. We use weak fields and make sure we probe the linear response regime (see SM for details).

Self-energy approximation—We compute the self-energy perturbatively in powers of U, and truncate at second order. The first-order self-energy in the Hubbard model is instantaneous (the Hartree shift) and can be absorbed in the single-particle Hamiltonian h. What remains to be computed is a single Feynman diagram,

$$\Sigma_{ij}(t,t')[G]=U^2G_{ij}(t,t')G_{ij}(t,t')G_{ji}(t',t). \qquad (5)$$

However, one may still choose to compute the diagram self-consistently or not, i.e., the propagator appearing in the self-energy diagram can be considered to be the fully dressed propagator (G) or the bare propagator (G_0). The self-consistent approximation corresponds to an approximation of the Luttinger-Ward functional and is guaranteed to respect charge and energy conservation laws. The two approximations for the self-energy must become indistinguishable as $U\to 0$, but at any finite U, they may yield different results.

Results—Our nonequilibrium theory is illustrated in an example in Fig. 1. We find that the three protocols yield perfectly consistent results [e.g., in Figs. 1(a) and 1(c) we show in red the comparison to the protocol (b) result]. However, the two self-energy approximations lead to drastically different results. Most importantly, the $\Sigma[G_0]$ approximation yields infinite conductivity. This manifests differently in the three different protocols. In the case of constant electric field, this means there is no stationary state and the current keeps growing with time. In the short electric field pulse case, the current does not decay to zero, but to a finite constant instead [as shown on Fig. 1(a), the constant is in perfect agreement with the slope of the linear growth of the current in the protocol (a)]. This indicates that the infinite conductivity is due to a finite charge stiffness D, which is when the optical conductivity can be separated in two parts as $\sigma(t)=\sigma^{\rm reg}(t)+D\theta(t)$, with the regular part $\sigma^{\rm reg}(t)$ decaying to zero at long times [60,61]. In frequency domain this means ${\rm Re}\sigma(\omega)=\pi D\delta(\omega)+{\rm Re}\sigma^{\rm reg}(\omega)$. In the short vector potential pulse case, the current does decay to zero, but the charge stiffness can be deduced from the obtained current-current correlation function based on the relation $\int_0^\infty {\rm d}t\Lambda(t)=K-D$. Regardless of the Σ approximation, the optical sum rule $\sigma(t=0^+)=K=(1/\pi)\int{\rm d}\omega{\rm Re}\sigma(\omega)$ is satisfied [Fig. 1(b), SM]. To confirm that our results indicate charge stiffness, rather than a large conductivity, we have studied how $\sigma(\omega)$ changes in the presence of a small fermionic bath (see SM).

Cross-checking with RFDiagMC—To cross-check the nonequilibrium results, we employ our new implementation of the RFDiagMC method for the computation of correlation functions in equilibrium. To do this, we first need to determine the diagrammatic content of the current-current correlation function that we effectively compute in our nonequilibrium calculations (in principle, in neither the $\Sigma[G_0]$ nor the $\Sigma[G]$ case will the diagrammatic content correspond to the bold perturbation theory for the current-current correlation function). Given an approximation for the self-energy, one can express the generalized two-particle susceptibility χ as a functional derivative of the Green's function with respect to an applied external field, $\chi=(\delta G/\delta\phi)$ [62]. In the case of the $\Sigma[G]$ approximation, this yields the self-consistent Bethe-Salpeter equation, with χ appearing on both sides of the equation. In the case of $\Sigma[G_0]$, one finds a closed expression where the

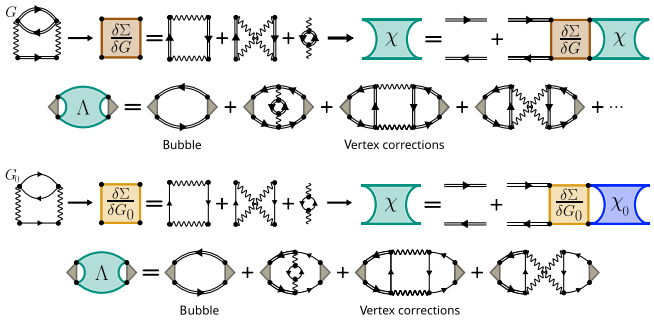

FIG. 2. Diagrammatic content of the current-current correlation function effectively computed in our nonequilibrium theory based on different diagrammatic approximations for the self-energy.

noninteracting $\chi_0 = G_0 G_0$ appears on the rhs instead. The current-current correlation function Λ is obtained by connecting the legs of the generalized susceptibility χ to two current vertices v. We see that in the case of $\Sigma[G]$, Λ effectively contains infinitely many skeleton diagrams of all even orders with all propagators being the full Green's functions. Up to second order, all nonzero bold-skeleton diagrams are captured. However, odd orders are not captured, and at order 4 and above not all skeleton diagrams are captured. In the $\Sigma[G_0]$ case, one obtains only three second-order diagrams, which are skeleton, but all propagators except two are bare. See Fig. 2 and SM for details.

The Λ diagrams from Fig. 2 can be computed using RFDiagMC, and we denote these theories as $\Sigma[G]$ and $\Sigma[G_0]$. The comparison with nonequilibrium results is then made by comparing $\sigma^{\mathrm{reg}}(\omega)$ and D. Both can be computed from Λ, namely $\mathrm{Re}\sigma^{\mathrm{reg}}(\omega \neq 0) = \mathrm{Im}\,\Lambda(\omega)/\omega$, $\sigma^{\mathrm{reg}}_{\mathrm{dc}} = [\partial\,\mathrm{Im}\,\Lambda(\omega)/\partial\omega]|_{\omega\to 0}$ and $D = K - \mathrm{Re}\Lambda(\omega = 0)$. The results are presented in Fig. 3(a). We see excellent agreement. In the case of $\Sigma[G]$ effective Λ diagrams, it was enough to do only second-order vertex correction diagrams to reach agreement, which means that fourth and higher order diagrams are all negligible. In the case of $\Sigma[G]$, the charge stiffness was found to be below statistical error. In the case of $\Sigma[G_0]$, the charge stiffness entirely comes from vertex corrections.

Perturbation theory for Λ—Now that we have established the validity of our implementation, we can also use RFDiagMC to solve the perturbation theory for the current-current correlation function. We take a given self-energy approximation, construct the dressed Green's function, and then compute *all* the bold-skeleton diagrams, up to a given order (including the odd orders). We denote such theories as Λ-pert. with a given Σ approximation. We find that third-order diagrams are practically negligible at $U = 0.1$ (see SM), and the series is most likely converged already at second order. Therefore, our Λ-pert. $\Sigma[G]$ theory gives the same result as the noneq. $\Sigma[G]$ theory. However, the Λ-pert. $\Sigma[G_0]$ approximation is different from the nonequilibrium $\Sigma[G_0]$ theory because the vertex correction diagrams we compute are different. The results for all three distinct theories (as well as the Boltzmann theory) are compared in Fig. 3(b).

Discussion and prospects for future work—We observe a clear trend that Λ-pert. $\Sigma[G_0]$ and $\Sigma[G]$ results become the same as $U \to 0$ [Fig. 3(b)]. This indicates that the Λ-pert.

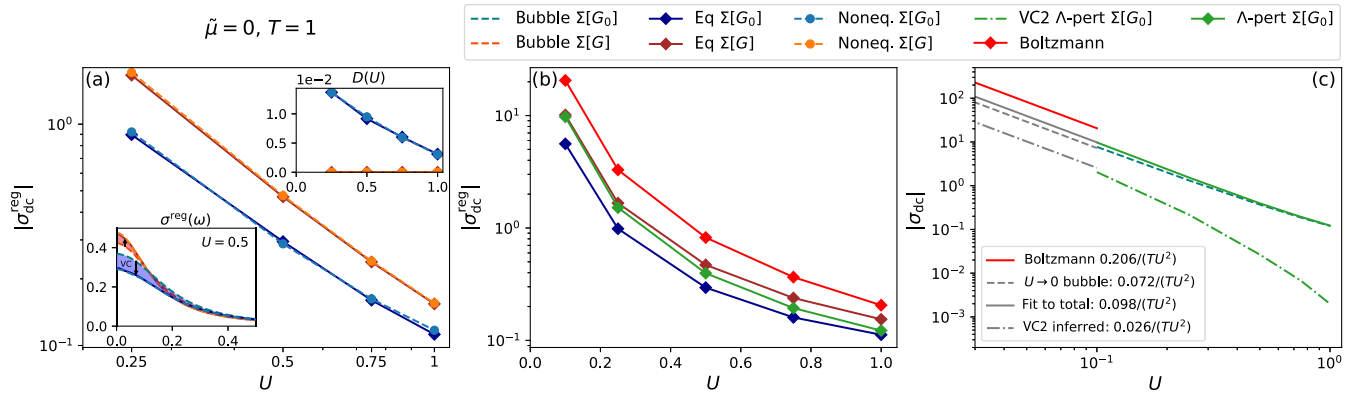

FIG. 3. Main results showing the comparison between different theories and the divergence of vertex corrections in the $U \to 0$ limit. (a) Cross-check between equilibrium and the corresponding nonequilibrium theories showing perfect agreement in terms of the regular part of the dc conductivity $\sigma^{\mathrm{reg}}_{\mathrm{dc}}$ (main panel), optical conductivity $\mathrm{Re}\sigma^{\mathrm{reg}}(\omega)$ (lower inset), and the charge stiffness D (upper inset). The lower inset also shows the contribution of the vertex corrections to $\mathrm{Re}\sigma^{\mathrm{reg}}(\omega)$ (positive in $\Sigma[G]$ approximation, negative in $\Sigma[G_0]$ approximation, vanishing at high frequency). (b) Comparison between two possible Λ-perturbation (Λ-pert.) theories (brown and green), the theory consistent with nonequilibrium (noneq.) $\Sigma[G_0]$ approximation (blue), and the Boltzmann theory(red), showing that different Λ-pert. theories become indistinguishable as $U \to 0$, while the noneq. $\Sigma[G_0]$ and the Boltzmann remain different. (c) Small-U scaling of the results. Gray lines display the strict $U \to 0$ scaling: the dashed gray line denotes the bubble computed in this limit, using the approach explained in [45]; the full gray line is a fit to the total result (full green line); the dash-dotted line is inferred from the previous two; the scaling of Boltzman results is taken from [46].

series is not sensitive to the precise choice of the Σ approximation—as our second-order $\Sigma[G]$ and $\Sigma[G_0]$ converge in the weak-coupling limit, so do the corresponding low-order bold-skeleton perturbation theories for Λ. However, we observe that (non)eq. $\Sigma[G_0]$ and Boltzmann theory results remain different as $U \to 0$.

To understand this, it is important to note that the Λ diagrams that are effectively being computed in our noneq. $\Sigma[G_0]$ theory do not form a proper low-order perturbation theory. Even though $\Sigma[G_0]$ becomes exact as $U \to 0$ (and is even expected to perform best at low but finite coupling [63,64]; see also SM), the current response one gets from it is most likely never exact, no matter how low the value of U. The vertex corrections introduced this way subtract from $\sigma_{\mathrm{dc}}^{\mathrm{reg}}$, which is opposite to what is found in noneq. $\Sigma[G]$ and the previous work with FTLM [24]. The failure of $\Sigma[G_0]$ is relevant for Ref. [48] where in a similar theory, at low doping and high temperature, vertex corrections are also found to suppress dc conductivity instead of enhance it (see SM).

On the other hand, the Boltzmann theory is equivalent to our noneq. $\Sigma[G]$ theory, plus additional approximations. Most importantly, the Green's function appearing in the collision integral and the second-order self-energy is simplified by the quasiparticle approximation (leading to expressions formally similar to our $\Sigma[G_0]$; see SM for details). Therefore, the Boltzmann theory cannot be more accurate than our noneq. $\Sigma[G]$ theory, and the additional approximations likely lead to the quantitatively wrong scaling we observe at $U \to 0$.

Our main finding is that the vertex corrections to dc conductivity do not vanish, even as $U \to 0$. It appears that both the bubble and the vertex corrections diverge at small U as $1/U^2$, but with a different prefactor, meaning that, as U is reduced, the ratio between the bubble and the vertex corrections remains fixed. This happens despite the U^2 prefactor in second-order vertex correction diagrams (VC2). The reason is that the frequency dependence $\mathrm{Im}\,\Lambda^{\mathrm{VC2}}(\omega)/U^2$ becomes singular at $\omega = 0$ as $U \to 0$ (we have checked this by computing Λ diagrams with the bare propagators; see SM). It is possible that a similar scenario happens at higher orders as well, and that *all orders* of perturbation contribute to σ_{dc} even at infinitesimal coupling. Our results, however, suggest that third-order vertex corrections to σ_{dc} at $U = 0.1$ are at least 2 orders of magnitude smaller than second order. At $U \approx 0.1$–0.25, the difference between Λ-pert. $\Sigma[G]$ and Λ-pert. $\Sigma[G_0]$ results appears to be only due to the difference in the self-energy, not due to lack of convergence of the Λ series.

Our findings show that neither the Boltzmann theory nor the Kubo bubble are exact in the weak-coupling limit. To fully confirm the strange-metal phenomenology that these two theories predict at $U \to 0$ and half-filling [45], we need to be able to do calculations at temperatures of order 0.001–0.1. This will require further optimization in both our RFDiagMC and noneq. $\Sigma[G]$ theories, which are currently limited to about $T > 0.05$. Our nonequilibrium approach can be pushed to lower temperatures by using compression methods [65,66], and the preliminary results are encouraging. With additional optimization outside of the scope of the current Letter, we should also be able to push RFDiagMC to lower temperatures and stronger coupling. The path forward is clear, at least in principle: one should attempt to converge the bare series for the equilibrium $\Sigma[G_0]$, then use it to dress the Green's function, and then try to converge the bold-skeleton series for Λ.

Computations were performed on the PARADOX supercomputing facility (Scientific Computing Laboratory, Center for the Study of Complex Systems, Institute of Physics Belgrade).

Acknowledgments—We acknowledge useful discussions with Hugo Strand, Nenad Vukmirović, Rok Žitko, Antoine Georges, André-Marie Tremblay, and Jéróme Leblanc. The authors also acknowledge the access granted to the HPC resources of TGCC and IDRIS under the allocations A0170510609 attributed by GENCI (Grand Equipement National de Calcul Intensif) and to the high performance computing resources of IDCS (Infrastructure, Données, Calcul Scientifique) under the allocation CPHT 2024. J. V. and J. K. acknowledge funding provided by the Institute of Physics Belgrade, through a grant by the Ministry of Science, Technological Development and Innovation of the Republic of Serbia. J. V. and J. K. acknowledge funding by the European Research Council, Grant No. ERC-2022-StG:101076100.

Data availability—The data that support the findings of this article are not publicly available upon publication because it is not technically feasible and/or the cost of preparing, depositing, and hosting the data would be prohibitive within the terms of this research project. The data are available from the authors upon reasonable request.

[1] B. Keimer, S. A. Kivelson, M. R. Norman, S. Uchida, and J. Zaanen, Nature (London) **518**, 179 (2015).
[2] P. Limelette, P. Wzietek, S. Florens, A. Georges, T. A. Costi, C. Pasquier, D. Jérome, C. Mézière, and P. Batail, Phys. Rev. Lett. **91**, 016401 (2003).
[3] Y. Kurosaki, Y. Shimizu, K. Miyagawa, K. Kanoda, and G. Saito, Phys. Rev. Lett. **95**, 177001 (2005).
[4] F. Kagawa, K. Miyagawa, and K. Kanoda, Nature (London) **436**, 534 (2005).
[5] M. Dumm, D. Faltermeier, N. Drichko, M. Dressel, C. Mézière, and P. Batail, Phys. Rev. B **79**, 195106 (2009).
[6] B. J. Powell and R. H. McKenzie, Rep. Prog. Phys. **74**, 056501 (2011).
[7] T. Furukawa, K. Miyagawa, H. Taniguchi, R. Kato, and K. Kanoda, Nat. Phys. **11**, 221 (2015).
[8] E. Y. Andrei and A. H. MacDonald, Nat. Mater. **19**, 1265 (2020).

[9] Y. Cao, D. Chowdhury, D. Rodan-Legrain, O. Rubies-Bigorda, K. Watanabe, T. Taniguchi, T. Senthil, and P. Jarillo-Herrero, Phys. Rev. Lett. **124**, 076801 (2020).

[10] T. Li, S. Jiang, L. Li, Y. Zhang, K. Kang, J. Zhu, K. Watanabe, T. Taniguchi, D. Chowdhury, L. Fu, J. Shan, and K. F. Mak, Nature (London) **597**, 350 (2021).

[11] H. Takagi, B. Batlogg, H. L. Kao, J. Kwo, R. J. Cava, J. J. Krajewski, and W. F. Peck, Phys. Rev. Lett. **69**, 2975 (1992).

[12] R. A. Cooper, Y. Wang, B. Vignolle, O. J. Lipscombe, S. M. Hayden, Y. Tanabe, T. Adachi, Y. Koike, M. Nohara, H. Takagi, C. Proust, and N. E. Hussey, Science **323**, 603 (2009).

[13] A. Legros, S. Benhabib, W. Tabis, F. Laliberté, M. Dion, M. Lizaire, B. Vignolle, D. Vignolles, H. Raffy, Z. Z. Li, P. Auban-Senzier, N. Doiron-Leyraud, P. Fournier, D. Colson, L. Taillefer, and C. Proust, Nat. Phys. **15**, 142 (2018).

[14] R. Krishna Kumar, X. Chen, G. H. Auton, A. Mishchenko, D. A. Bandurin, S. V. Morozov, Y. Cao, E. Khestanova, M. Ben Shalom, A. V. Kretinin, K. S. Novoselov, L. Eaves, I. V. Grigorieva, L. A. Ponomarenko, V. I. Fal'ko, and A. K. Geim, Science **357**, 181 (2017).

[15] R. K. Kumar, A. Mishchenko, X. Chen, S. Pezzini, G. H. Auton, L. A. Ponomarenko, U. Zeitler, L. Eaves, V. I. Fal'ko, and A. K. Geim, Proc. Natl. Acad. Sci. U.S.A. **115**, 5135 (2018).

[16] C. G. Wang, R. Zhou, and G.-q. Zheng, in *Proceedings of the International Conference on Strongly Correlated Electron Systems (SCES2019)* (Physical Society of Japan, Tokyo, 2020), 10.7566/JPSCP.30.011028.

[17] G. Grissonnanche, Y. Fang, A. Legros, S. Verret, F. Laliberté, C. Collignon, J. Zhou, D. Graf, P. A. Goddard, L. Taillefer, and B. J. Ramshaw, Nature (London) **595**, 667 (2021).

[18] A. Jaoui, I. Das, G. Di Battista, J. Díez-Mérida, X. Lu, K. Watanabe, T. Taniguchi, H. Ishizuka, L. Levitov, and D. K. Efetov, Nat. Phys. **18**, 633 (2022).

[19] J. Ayres, M. Berben, M. Čulo, Y.-T. Hsu, E. van Heumen, Y. Huang, J. Zaanen, T. Kondo, T. Takeuchi, J. R. Cooper, C. Putzke, S. Friedemann, A. Carrington, and N. E. Hussey, Nature (London) **595**, 661 (2021).

[20] S. A. Grigera, R. S. Perry, A. J. Schofield, M. Chiao, S. R. Julian, G. G. Lonzarich, S. I. Ikeda, Y. Maeno, A. J. Millis, and A. P. Mackenzie, Science **294**, 329 (2001).

[21] J. Vučičević, D. Tanasković, M. J. Rozenberg, and V. Dobrosavljević, Phys. Rev. Lett. **114**, 246402 (2015).

[22] P. Cha, N. Wentzell, O. Parcollet, A. Georges, and E.-A. Kim, Proc. Natl. Acad. Sci. U.S.A. **117**, 18341 (2020).

[23] J. Kokalj, Phys. Rev. B **95**, 041110 (2017).

[24] J. Vučičević, J. Kokalj, R. Žitko, N. Wentzell, D. Tanasković, and J. Mravlje, Phys. Rev. Lett. **123**, 036601 (2019).

[25] I. Vasić and J. Vučičević, Phys. Rev. B **110**, 064501 (2024).

[26] M. Rigol, T. Bryant, and R. R. P. Singh, Phys. Rev. Lett. **97**, 187202 (2006).

[27] E. Khatami and M. Rigol, Phys. Rev. A **84**, 053611 (2011).

[28] B. Tang, E. Khatami, and M. Rigol, Comput. Phys. Commun. **184**, 557 (2013).

[29] D.-W. Qu, Q. Li, S.-S. Gong, Y. Qi, W. Li, and G. Su, Phys. Rev. Lett. **133**, 256003 (2024).

[30] P. J. H. Denteneer, R. T. Scalettar, and N. Trivedi, Phys. Rev. Lett. **83**, 4610 (1999).

[31] E. W. Huang, R. Sheppard, B. Moritz, and T. P. Devereaux, Science **366**, 987 (2019).

[32] F. Šimkovic, R. Rossi, A. Georges, and M. Ferrero, Science **385**, 6715 (2024).

[33] M. Schiró, Phys. Rev. B **81**, 085126 (2010).

[34] G. Cohen, E. Gull, D. R. Reichman, and A. J. Millis, Phys. Rev. Lett. **115**, 266802 (2015).

[35] R. E. V. Profumo, C. Groth, L. Messio, O. Parcollet, and X. Waintal, Phys. Rev. B **91**, 245154 (2015).

[36] M. Maček, P. T. Dumitrescu, C. Bertrand, B. Triggs, O. Parcollet, and X. Waintal, Phys. Rev. Lett. **125**, 047702 (2020).

[37] C. Bertrand, D. Bauernfeind, P. T. Dumitrescu, M. Maček, X. Waintal, and O. Parcollet, Phys. Rev. B **103**, 155104 (2021).

[38] A. Auerbach, Phys. Rev. B **99**, 115115 (2019).

[39] I. Khait, S. Bhattacharyya, A. Samanta, and A. Auerbach, npj Quantum Mater. **8**, 75 (2023).

[40] M. Qin, T. Schäfer, S. Andergassen, P. Corboz, and E. Gull, Annu. Rev. Condens. Matter Phys. **13**, 275 (2022).

[41] H. Terletska, J. Vučičević, D. Tanasković, and V. Dobrosavljević, Phys. Rev. Lett. **107**, 026401 (2011).

[42] X. Deng, J. Mravlje, R. Žitko, M. Ferrero, G. Kotliar, and A. Georges, Phys. Rev. Lett. **110**, 086401 (2013).

[43] J. Vučičević and R. Žitko, Phys. Rev. Lett. **127**, 196601 (2021).

[44] H. Xu, H. Shi, E. Vitali, M. Qin, and S. Zhang, Phys. Rev. Res. **4**, 013239 (2022).

[45] J. Vučičević, S. Predin, and M. Ferrero, Phys. Rev. B **107**, 155140 (2023).

[46] T. G. Kiely and E. J. Mueller, Phys. Rev. B **104**, 165143 (2021).

[47] U. Schneider, L. Hackermüller, J. P. Ronzheimer, S. Will, S. Braun, T. Best, I. Bloch, E. Demler, S. Mandt, D. Rasch, and A. Rosch, Nat. Phys. **8**, 213 (2012).

[48] D. Bergeron, V. Hankevych, B. Kyung, and A.-M. S. Tremblay, Phys. Rev. B **84**, 085128 (2011).

[49] J. Vučičević, P. Stipsić, and M. Ferrero, Phys. Rev. Res. **3**, 023082 (2021).

[50] J. Vučičević and M. Ferrero, Phys. Rev. B **101**, 075113 (2020).

[51] A. Taheridehkordi, S. H. Curnoe, and J. P. F. LeBlanc, Phys. Rev. B **99**, 035120 (2019).

[52] M. Grandadam and J. P. F. LeBlanc, arXiv:2303.04964.

[53] I. Sobol', USSR Computational Mathematics and Mathematical Physics **7**, 86 (1967).

[54] H. U. R. Strand, J. Kleinhenz, and I. Krivenko, Phys. Rev. B **110**, L121120 (2024).

[55] M. Schüler, D. Golež, Y. Murakami, N. Bittner, A. Herrmann, H. U. Strand, P. Werner, and M. Eckstein, Comput. Phys. Commun. **257**, 107484 (2020).

[56] See Supplemental Material at http://link.aps.org/supplemental/10.1103/mm38-zttx for details.

[57] H. Aoki, N. Tsuji, M. Eckstein, M. Kollar, T. Oka, and P. Werner, Rev. Mod. Phys. **86**, 779 (2014).

[58] J. Vučičević and R. Žitko, Phys. Rev. B **104**, 205101 (2021).

[59] A. Amaricci, C. Weber, M. Capone, and G. Kotliar, Phys. Rev. B **86**, 085110 (2012).

[60] D. M. Kennes, E. Y. Wilner, D. R. Reichman, and A. J. Millis, Phys. Rev. B **96**, 054506 (2017).
[61] T. Kaneko, S. Yunoki, and A. J. Millis, Phys. Rev. Res. **2**, 032027(R) (2020).
[62] G. Baym and L. P. Kadanoff, Phys. Rev. **124**, 287 (1961).
[63] E. Kozik, M. Ferrero, and A. Georges, Phys. Rev. Lett. **114**, 156402 (2015).
[64] J. Gukelberger, L. Huang, and P. Werner, Phys. Rev. B **91**, 235114 (2015).
[65] J. Kaye and D. Golež, SciPost Phys. **10**, 091 (2021).
[66] J. Kaye and H. U. R. Strand, Adv. Comput. Math. **49**, 63 (2023).